Jurnal Teknologi

Full Paper

SIMULATION STUDY ON ENHANCING HYDROGEN PRODUCTION IN AN OCEAN THERMAL ENERGY (OTEC) SYSTEM UTILIZING A SOLAR COLLECTOR

Amyra MY[a], Nor Azizi Othman[a*], Shamsul Sarip[b,d], Yasuyuki Ikegami[d,e], Mohd Alshafiq Tambi Chik[a], Norazli Othman[b], Ridzuan Yacob[c], Hirofumi Hara[a,e], Zuriati Zakaria[a]

[a]Malaysia-Japan International Institute of Technology, Universiti Teknologi Malaysia ,K. Lumpur, Malaysia
[b]Institute of Ocean Energy, Universiti Teknologi Malaysia
[c]School of Business & Management Maritime, Universiti Malaysia Terengganu, Malaysia
[d]Razak School of Engineering and Advanced Technology, Universiti Teknologi Malaysia, K. Lumpur, Malaysia
[e]Institute of Ocean Energy, Saga University, Saga, Japan

*Corresponding author
azizicitycampus@gmail.com

Graphical abstract
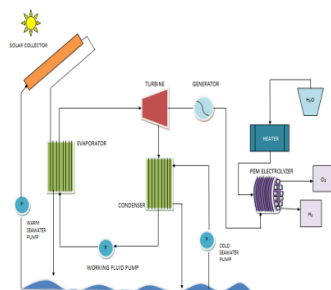
Abstract

This article reports the simulation study on the performance of utilizing a solar collector at the inlet of an evaporator to provide auxiliary heat into a system for hydrogen generation in an OTEC cycle. The conventional method of OTEC is simulated by FORTRAN programming and the results were compared with the presence of solar collector on the system. In the simulation experimental, the incoming temperature of warm seawater was boosted by using a flat plate solar collector. For the purpose of the experiment, a 100 kW OTEC cycle that was designed incorporated a solar boosting capability. Its thermodynamic efficiency was then compared through a series of simulation involving several control parameters. The results reveal that the proposed solar boosted OTEC enhanced the thermal efficiency, T_E. Increase in solar power absorption can increase the net power output, thus increasing the amount of hydrogen produced. The results obtained provided insights, from a thermodynamic perspective, on the outcome of combining sustainable energy with solar thermal energy to improve the system performance.

Keywords: Solar collector, ocean thermal energy, hydrogen production, power generation, solar energy

Abstrak

Artikel ini melaporkan kajian simulasi kepada prestasi menggunakan pengumpul suria pada kemasukan penyejat yang menyediakan haba tambahan ke dalam sistem untuk penjanaan hidrogen dalam kitaran OTEC. Simulasi melaui kaedah pengaturcaraan FORTRAN telah dijalankan ke atas model konvensional OTEC dan keputusan yang terhasil dibandingkan dengan keputusan kehadiran pengumpul suria pada sistem. Dalam simulasi eksperimen, suhu air panas yang masuk telah dinaikkan oleh pengumpul suria plat rata. Bagi tujuan percubaan, 100 kW kitaran OTEC telah direka dengan keupayaan meningkatkan solar. Kecekapan termodinamik kemudian dibanding melalui satu siri simulasi yang melibatkan beberapa parameter kawalan. Keputusan menunjukkan bahawa solar yang dicadangkan merangsang prestasi OTEC dan peningkatan kecekapan haba, TE. Peningkatan penyerapan tenaga solar boleh meningkatkan output kuasa bersih, sekaligus meningkatkan jumlah hidrogen dihasilkan. Keputusan yang

diperolehi diberikan pandangan dari perspektif termodinamik, mengenai hasil gabungan tenaga lestari dengan tenaga haba solar untuk meningkatkan prestasi sistem.

Kata kunci: Pengumpul suria, ocean thermal energy, pengeluaran hidrogen, penjanaan kuasa, tenaga solar

1.0 INTRODUCTION

Ocean thermal energy conversion is a technology that utilizes the concept of temperature difference between hot surface seawater and cold deep seawater to generate electricity. A lot of effort has been made related to ocean thermal energy conversion since it first proposed by French physicist D'Arsonval in 1881. Due to the small temperature difference, the main technical challenge faced by OTEC is the low energy conversion efficiency. The temperature difference between hot surface seawater and cold deep seawater even in the tropical area is only 20-25°C. Although OTEC required abundant of seawater flow rates, the best thermodynamic efficiency achieved lies in the range 3-5%[1]. The net power efficiency can be defined as net power divided by generated power. In a typical OTEC plant the net power efficiency is between 50-80% of the system. Many considerable research efforts have been made to improve the performance of the OTEC system. The first research area has been aimed at increasing the efficiency of OTEC cycle by thermodynamic optimization [2, 3].

Tong *et al*. studied the performance of CC-OTEC system with the additional solar collector at the outlet of evaporator. They have determined the most suitable working fluid and found that the appropriate net power of the cycle should be at least 50 kW [2]. Yeh *et al*. has theoretically investigated the dependent parameter on the net power output of OTEC to generate a maximum net power [3]. The optimization of a closed-cycle OTEC system was studied with the plate type heat exchanger using ammonia as working fluid by the Powell method [4]. Pouri *et al*. has reported the exergy and energy analysis of hydrogen production in a solar preheated OTEC cycle. This research focused on the effect of solar radiation on the exergy destruction rate and exergy efficiency [5]. Yamada *et al*. has carried out the simulation of 20 K and 40 K boosted temperature at the outlet of evaporator by preheated solar to generate 100 kW of SOTEC plant and investigating the solar collector area needed at different types of solar collector [6]. Straatman and Van Sart [7] experimented using a variation of the OTEC where the OTEC is combined with an offshore solar pond which they had referred to as a hybrid system(OTEC-OSP). Aashay Tinaikar *et al.* [8] utilized a superheated and preheated black metallic plate of aluminium which were used to compensate the heat losses in the heat exchanger. This study also lists out the benefits and drawbacks from the proposed OTEC plant. Besides the Rankine cycle, there are two more types of OTEC cycles, namely Uehara [9]

and Kalina [10] cycles, both of which are also suitable for use to generate electricity from OTEC plant. These studies have focused on the design of solar-boosted OTEC systems, suggesting the construction of a new power plant operating at a much higher pressure ratio than the conventional OTEC system.

However, OTEC power plants demand huge initial construction costs (e.g., ~ $ 1.6B for a 100 MW OTEC power plant [11] due to the need to have enormous seawater mass flow rates and corresponding heat exchanger and seawater piping sizes. It would be more economically feasible to consider improving OTEC plants by adding solar thermal collection on top of existing power-generating and piping components. Many studies were performed to analyze the importance and benefits of hydrogen energy, especially for the next generation. The projected increase in human population is expected to be accompanied by an increase in the demand for hydrogen, particularly for use in transportation, food, medicines, chemicals and others [12]. Greenhouse gases (GHG) emitted to environment is a result of increased energy and food demand. To reduce the GHG emissions into the air, the method of hydrogen production must be from sustainable energy source, now often referred to as green hydrogen production method. Hydrogen energy systems appear to be one of the most effective solutions and can play a significant role in providing better environment and sustainability[13]

The research is aimed at studying the performance of boosted solar OTEC on hydrogen production under Malaysian conditions. In this study, a solar collector is simply installed to the conventional OTEC component to provide auxiliary heat to the system and increase the thermodynamic efficiency. The performance simulation of a 100kW of boosted solar OTEC is carried out based on Malaysia temperature condition. Then, the simulation results obtained are compared with that of the conventional OTEC plant. The performance of the proposed solar boosted OTEC system is studied by looking at the effects of several pre-identified control parameters.

2.0 EQUATION AND CONDITION FOR SIMULATION

2.1 Solar Energy Analysis

The useful heat gained by seawater or fluid Q_u is given by the equation

$$Q_u = mc_p (\dot{T}_{out} - T_{in}) \tag{1}$$

Where T_{in} and T_{out} are inlet and outlet seawater temperature of solar collector, m is the mass flow rate and c_p is the specific heat. The useful heat gained by flat plate solar collector as given by Hottle-Whillier equation is

$$Q_u = A_p F_R [S - \dot{U}_1(T_{in} - T_o)] \tag{2}$$

Where T_o is the ambient temperature, F_R is heat removal factor that is defined as:

$$F_R = \frac{\dot{m} \, C_p}{U_1 \, A_p} [1 - e^{\{-\frac{F'U_1 A_p}{\dot{m} C_p}\}}] \tag{3}$$

Where the F' is collector efficiency factor with a value of 0.914 and U_1 the overall loss coefficient.
Radiation flux can be calculated as:

$$S = (\alpha\tau)I \tag{4}$$

Where $(\alpha\tau)$ is the optical efficiency and I is a solar radiation intensity. The energy efficiency of the solar flat plate collector is expressed as:

$$\eta = \frac{Q_u}{IA_p} \tag{5}$$

2.2 Organic Rankine Cycle

In the evaporator, a working fluid is evaporated to saturated vapor by receiving heat from the warm seawater. The energy balance equation at each side of the evaporator can be written as:

$$Q_E = m_{ws}c_{p,ws}(T_{wsi} - T_{wso}) = m_{wf}(h_1 - h_4) \tag{6}$$

With the assumption that seawater is an ideal incompressible fluid. Enthalpy and entropy of the working fluid, which are in general a function of pressure and vapor quality during phase change were determined from PROPATH.
  Overall heat transfer coefficient and effective surface area of the evaporator correlates with the heat addition rate as shown in the following equation:

$$Q_E = U_E A_E \Delta T_{lm,E} \tag{7}$$

Where $\Delta T_{lm,E}$ is the logarithmic mean temperature difference across the evaporator, and the effective thermal conductance $U_E A_E$ can be approximately as

$$\frac{1}{U_E A_E} = \frac{1}{h_{wf} A_E} + \frac{1}{h_{ws} A_E} \tag{8}$$

Basically the energy balance equation for the condenser is same as that of the evaporator and is written as:

$$Q_C = m_{cs}c_{p,cs}(T_{cso} - T_{csi}) = m_{wf}(h_2 - h_3) \tag{9}$$

The heat transfer area of the condenser can be defined as below:

$$Q_C = U_C A_C \Delta T_{lm,C} \tag{10}$$

The logarithmic mean temperature difference across the evaporator and condenser is correlated as below:

For condenser,

$$\Delta T_{lm,C} = \frac{T_{cso} - T_{csi}}{ln\frac{T_c - T_{csi}}{T_c - T_{cso}}} \tag{11}$$

For evaporator,

$$\Delta T_{lm,E} = \frac{T_{wsi} - T_{wso}}{ln\frac{T_{wsi} - T_E}{T_{wso} - T_E}} \tag{12}$$

2.3 Turbine Generator Power

The turbine generator can be calculated from the product of mass working fluid flow rate, m_{wf} and the adiabatic heat loss across the turbine. The equation is as follows:

$$W_{T-G} = m_{wf} \, \eta_T \, \eta_G (h_2 - h_1) \tag{13}$$

Where, η_T and η_G are the turbine isentropic efficiency and generator mechanical efficiency which are assumed as having the values 0.9 and 0.95 respectively.

2.4 Warm Seawater Pumping Power

The warm seawater pumping power can be defined as follows:

$$W_{ws} = \frac{m_{ws}\Delta H_{ws}g}{\eta_{wsp}} \tag{14}$$

Where ΔH_{ws} is the total head difference of the warm seawater piping, m_{ws} is mass warm seawater flow rate, g is gravitational acceleration, 9.18ms^{-2} and η_{wsp} is efficiency of the warm seawater pump:

$$\Delta H_{ws} = (\Delta H_{ws})_P + (\Delta H_{ws})_E \tag{15}$$

Where $(\Delta H_{ws})_P$ is the pump head of the warm seawater pipe due to friction, which given as,

$$(\Delta H_{ws})_P = (\Delta H_{ws})_{sp} + (\Delta H_{ws})_B \tag{16}$$

$(\Delta H_{ws})_{sp}$ is the friction loss in the straight pipe, while (ΔH_{ws}) is the friction loss due to bending pipe. To measure the losses, refer to the equation below:

$$(\Delta H_{ws})_{sp} = 6.82\frac{L_{ws}}{d_{ws}^{1.17}} \, x(\frac{V_{ws}}{C_{ws}})^{1.85} \quad , C_{ws} = 100 \tag{17}$$

$$(\Delta H_{ws})_B = \sum\lambda_m\frac{V_{ws}^2}{2g} \tag{18}$$

Here, L_{ws} is the length of the warm seawater pipe, d_{ws} is the warm seawater inner pipe diameter and v_{ws}

defined as the velocity of warm seawater inside the pipe.

$$(\Delta H_{ws})_E = \lambda_E \frac{V_{ws}^2}{2g} \frac{L_E}{(Deq)_w} \qquad (19)$$

$(\Delta H_{ws})_E$ is the pressure difference of warm seawater in the evaporator. L_E is the length of evaporator plate and D_{eq} is the equivalent diameter while λ_E is friction loss coefficient taken from Ref [14]:

$$D_{eq} = 2\sigma \qquad (20)$$

Where σ is clearance.

2.5 Cold Seawater Pumping Power

The pumping power of cold seawater can be expressed as:

$$W_{cs} = \frac{m_{cs}\Delta H_{cs}g}{\eta_{csp}} \qquad (21)$$

ΔH_{cs} is a total head loss of cold seawater piping.

$$\Delta H_{cs} = (\Delta H_{cs})_P + (\Delta H_{cs})_C + (\Delta H_{cs})_d \qquad (22)$$

$(\Delta H_{cs})_P$ is the pump head of the cold seawater pipe:

$$(\Delta H_{cs})_P = (\Delta H_{cs})_{sp} + (\Delta H_{cs})_B \qquad (23)$$

These are similar with terms in Eqs.(15) and (16). $(\Delta H_{cs})_C$ is the cold seawater pressure difference in the condenser.

$$(\Delta H_{cs})_C = \lambda_C \frac{V_{cs}^2}{2g} \frac{L_C}{(Deq)_c} \qquad (24)$$

Where L_C is the length of condenser plate and also D_{eq} is the equivalent diameter. The pressure difference caused by the density difference between the warm seawater surface and cold deep seawater is calculated as below:

$$(\Delta H_{cs})_d = L_{cs} - \frac{1}{\rho_{cs}} \left(\frac{1}{2} (\rho_{ws} + \rho_{cs}) L_{cs} \right) \qquad (25)$$

2.6 Net Power Generation

The net power output from the system be calculated based on this equation:

$$W_N = W_{T-G} - W_{P,wf} - W_{P,ws} - W_{P,cs} \qquad (26)$$

By considering turbine power and pump powers, the obtained net power allows the calculation of the net thermal efficiency:

$$\eta_{th} = W_N / Q_E \qquad (27)$$

Based on the definition of cycle efficiency, net cycle efficiency should be defined as the following expression:

$$\eta_{net} = \frac{W_N}{W_T} \qquad (28)$$

2.7 Rate of Hydrogen Production

The rate of hydrogen produced can be calculated using the equation given below. In the equation, q_{H2} is the rate of hydrogen generated, P_{out} is the output power from OTEC cycle and W_{elec} is the required electrical power needed by the electrolyzer to crack the water molecules. To produce 1 kg of H_2, it requires about 143 MJ of energy which is equivalent to 40 kWh of electrical power.

$$q_{H2,elec} = \frac{P_{out}}{W_{elec}} \qquad (29)$$

Therefore, in this study, W_{elec} is assumed to have the value of 40 kWh.

3.0 SIMULATION MODEL

In order to compare the performance of conventional OTEC and solar OTEC, a turbine-generator power of 100kW was numerically conducted using FORTRAN programming. The equations of each component were calculated by applying an iteratively method with initial assumptions of outlet of warm seawater and cold seawater. The pinch point temperature difference at evaporator and condenser were set on this study. The evaporator and condenser temperature were then used to calculate the saturation pressure and temperature of the working fluid by using PROPATH. Besides, the enthalpy, entropy and specific volume at each point can be obtained from this program (i.e. h_{1-4}, s_{1-4} and v_{1-4}) as well. Once all the value at each point are calculated, the energy values at evaporator, condenser and evaporator, i.e. Eqs. (6), (9) and (13) must be balance. Then, the calculation of mass warm seawater flow rate, cold seawater and working fluid, respectively were conducted. After specifying the flow rate of warm and cold seawater, the pumping power of cold seawater and warm seawater were determined by applying Eq. (14) until (25).

Figure 1 and 2 shows the schematic diagram of conventional closed-Rankine OTEC cycle and the proposed solar boosted OTEC cycle. These figures show the general arrangement of the heat exchangers, pumps, piping, turbine generator, solar collector and PEM electrolyzer. In Figure 2, a solar collector is utilized to provide auxiliary heat into the system. The add-on solar is installed to preheat the warm seawater before entering the evaporator. The heat absorbed from solar collector by warm seawater will then heat the working fluid caused the enthalpy drop across the turbine increase. A simulation of 100 kW solar boosted OTEC is carried out to see its performance and the results were then compared with that of a conventional OTEC plant. The effect of solar collector on hydrogen production was also investigated. Hydrogen has a significant advantage as it can be produced without pollution and this increases the feasibility of an OTEC plant system. The simulated results are presented to compare the improvement of the system performances in terms

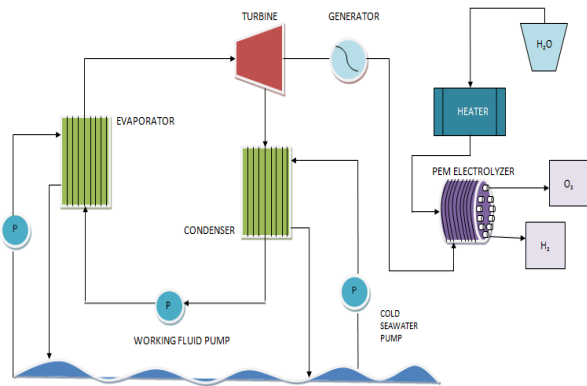of net thermal efficiency, net power output and solar collector area.

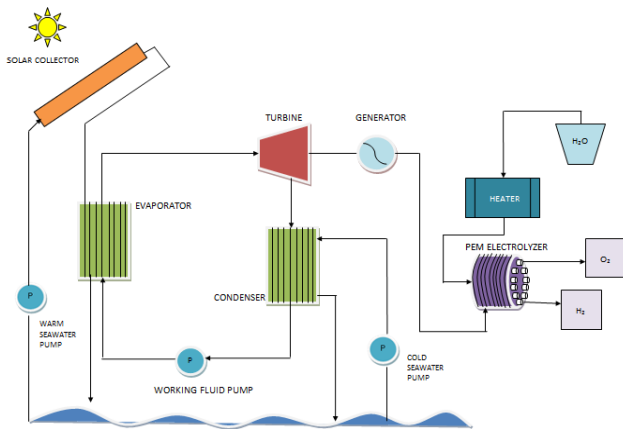**Figure 1** Schematic diagram of conventional OTEC cycle

Figure 2 Schematic diagram of solar boosted OTEC cycle

4.0 RESULTS AND DISCUSSION

Firstly, the conventional 100kW OTEC was simulated and the results of heat transfer areas of evaporator and condenser were determined. The results obtained were A_E =293.6 m^2 and A_C=318.2 m^2 respectively. In order to minimize the required heat transfer capacity to avoid exceeding the value obtained by conventional OTEC system, the flow rates of warm and cold sea water need to optimize. Table 1 is the initial condition that assumed to be constant for this simulation study. Table 2 shows the compilation results of a 100 kW OTEC and 100 kW solar boosted OTEC cycle. The results of 100 kW OTEC cycle indicated a good agreement with Ref [6] which also used a similar scale designed OTEC plant. The noticeable difference seen was due to the initial condition considered in this study. The results of a solar collector boost T_E by 20 K was also provided in this table. The theoretical thermal efficiency of a preheating solar OTEC showed an increment of 8.6%. This shows that adding on a solar plate into the system enables it to increase the net thermal efficiency by compensating for the losses of pumping power.

Table 1   Initial condition for the simulation

Turbine generator power, P_G	100	kW
Generator efficiency, η_G	0.96	-
Turbine efficiency, η_T	0.85	-
Efficiency of all pumps, (η_{WSP}, η_{CSP}, η_{WFP})	0.85	-
Evaporator (plate-type heat exchanger) Overall heat transfer coefficient (OTEC) T_{wsi}-T_E (BOOSTED OTEC) T_{sco}-T_E	4.0 4.1 4.1	kW/m^{2}K K K
Condenser (plate-type heat exchanger) Overall heat transfer coefficient T_C-T_{csi}	3.5 4.1	kW/m^{2}K K
Flat plate Solar Collector Tilt angle Azimuth angle	30 0	° °
Weather condition (Malaysia) Solar radiation Ambient temperature	800 25	W/m^2 °C
Temperature of sea water Warm sea water surface temperature (0 m) Cold deep sea water temperature (1000 m)	28 4	°C °C

Table 2 Simulation results of 100kW OTEC and 100kW solar boosted OTEC

			This study (OTEC)	Yamada et al.[6] (OTEC)	This study (Boosted 20K)
Warm sea water					
Inlet temperature	T_{wsi}	°C	28.0	25.7	28.0
Outlet temperature	T_{wso}	°C	25.1	22.9	45.1
Cold sea water					
Inlet temperature	T_{csii}	°C	4.0	4.4	4.0
Outlet temperature	T_{cso}	°C	6.8	7.1	6.8
Solar collector					
Inlet temperature	T_{sci}	°C	-	-	28.0
Outlet temperature	T_{sco}	°C	-	-	48.0
Evaporation temperature	T_E	°C	23.9	21.7	43.9
Condensation temperature	T_C	°C	8.1	8.4	8.1
Flow rate					
Warm sea water	m_{ws}	kg/s	203.8	260.0	99.2
Cold sea water	m_{cs}	kg/s	200.9	260.0	92.2
Working fluid	m_{wf}	kg/s	1.9	2.4	0.91
Net power	P_N	kW	71.0	69.9	85.9
Warm sea water pumping power	P_{ws}	kW	9.4	9.5	4.6
Cold sea water pumping power	P_{cs}	kW	17.7	18.6	8.1
Working fluid pumping power	P_{wf}	kW	1.9	2.1	1.4
Rankine cycle efficiency	η_R	-	4.2	3.4	8.7
Net Rankine cycle efficiency	η_{net}	-	3.0	2.3	7.5
Heat transfer area of evaporator	A_E	m²	293.6	231	142.9
Heat transfer area of condenser	A_c	m²	318.2	390	146.1
Flat plat solar collector					
Collector area	A_{SC}	m²	-	-	1678

Figure 3 shows the T-S and P-H diagram of solar boosted OTEC system. Point 1 is at saturated vapor, where at this point the working fluid is 100% in vapor state. Point 2 is located at the outlet of turbine and inlet of condenser, where the working fluid is a mixture of vapor and liquid. Point 2 is known as wet vapor state. Then, point 3 is a saturated liquid state (100% liquid of working fluid) and point 4 is a compressed liquid state which the points after the working fluid pump.

A solar boosted ocean thermal energy conversion (OTEC) was proposed to enhance the system performance with improvement in thermodynamic performance. In the preheated OTEC, the solar collector is installed at the inlet of evaporator with the function to preheat and provide additional heat to the warm seawater before entering the evaporator. Both results in Figure 4 and Figure 5, shows the effect of utilizing solar power absorption equivalent to 1000 kW.The maximum net power output from various readings of mass warm seawater flow rate was plotted as shown in the Figure 4. The graph shows that when mass warm seawater flow rate decreases, the net power output of the system is increases in line with the increase of inlet temperature of solar collector. However, when the mass of warm seawater flow rate continuously decrease, the value of net power cannot be read anymore. From the Eq. (1), the mass of warm seawater flow rate is inversely proportional to the inlet temperature of solar collector. Therefore, if the flow rate is decreased, the temperature will increase. However in this case, the maximum temperature of ammonia working fluid is 132°C. So, if the solar collector outlet temperature exceeded the maximum temperature of ammonia by lowering the flow rate of warm seawater, this is where the value of net power cannot be read any further. This is why in Figure 4 the net power output increased but then stopped at (Wnet=70 kW). This inefficient use of absorbed solar energy is because of limited surface area of the evaporator and condenser. Figure 5 shows the relationship of net power output and net efficiency of the solar boosted OTEC plant. Reducing the mass of warm seawater will increase the outlet temperature of solar collector. The larger the temperature difference between warm seawater and cold seawater, the larger will be the increase of the enthalpy drop across the turbine, drastically enhancing the net power generation of the system. Thus, decreasing the warm seawater flow rate will increase the net power output and net thermal efficiency as calculated by Eq. (28).
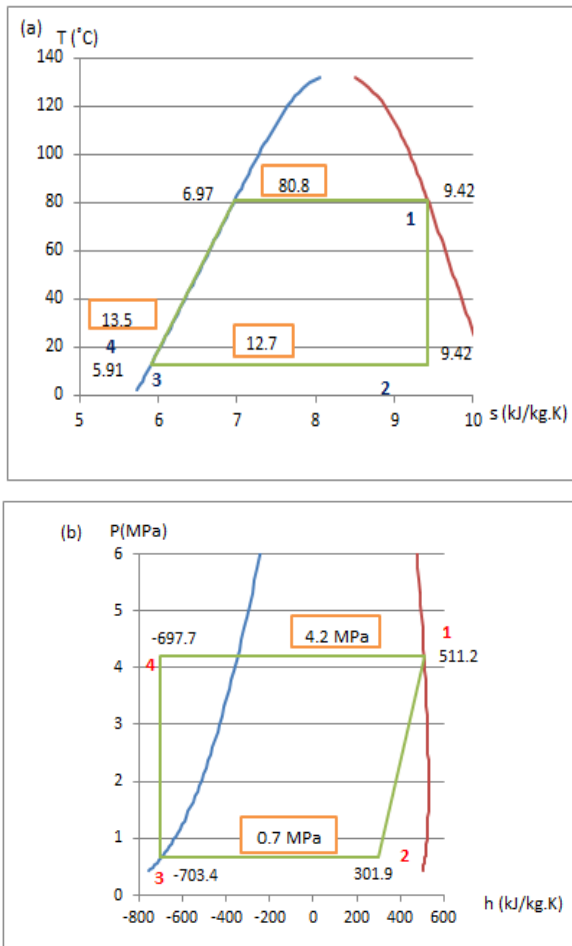
Figure 3 (a) T-S diagram of solar boosted OTEC system. (b) P-H diagram of solar boosted OTEC system of solar boosted OTEC system.

Figure 6 and Figure 7 show the simulation results for solar preheating OTEC. The various solar power absorption ranging from 1000 kW to 12000 kW were examined with the same mass warm seawater flow rate (i.e 30 kg/s) in the simulation process. The effect is seen on the net power generation. From the graph, the highest net power generation is achieved when the solar power absorption is 12000 kW. The increase in solar power absorption yields the increment of warm seawater temperature at the inlet of evaporator and resulting in a greater enthalpy drop across the turbine. When a larger solar power absorption is utilized, the inlet temperature of warm seawater is kept increasing, causing the temperature difference of warm seawater to increase. Figure 7 shows that increase in solar power absorption will increase the outlet temperature of the solar collector. From the result, to get 125°C of solar collector outlet temperature, it requires about 35000 m^2 of solar collector area with solar power absorption equivalent to 12 MW. As shown in Figure 7, the lowest solar power absorption is has the ability to increase the solar collector outlet to about 38°C, which is 10°C more that the inlet temperature of solar collector. Therefore,

the temperature difference between warm seawater and cold deep seawater can be increased beyond 20-25 °C by utilizing solar collector at the inlet of evaporator. The solar power absorption plays an important role in determining how much solar collector area is needed to achieve the required temperature. Obviously, the larger the solar collector area, the more capable it is to absorb more heat, resulting in an increase of the temperature of warm seawater at the inlet of the evaporator.
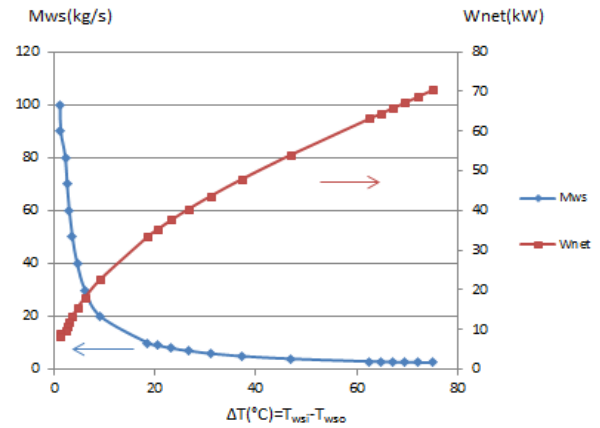

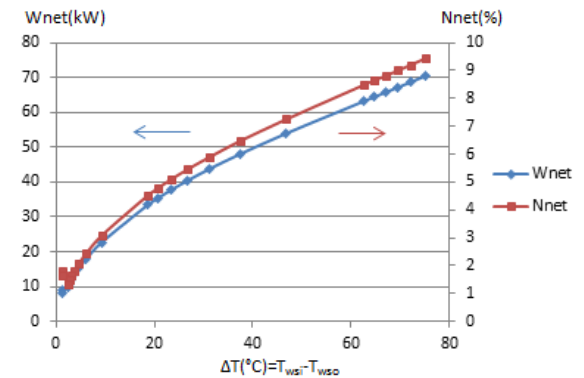**Figure 4** The relationship of net power output and mass warm seawater flow rate

Figure 5 The net power output as a function of net thermal efficiency. (Reducing mass warm seawater flow rate, Mws)
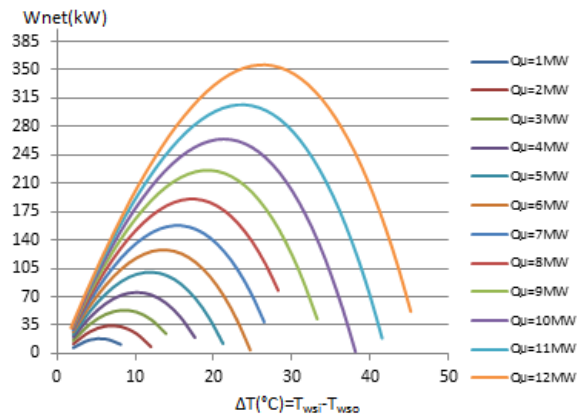

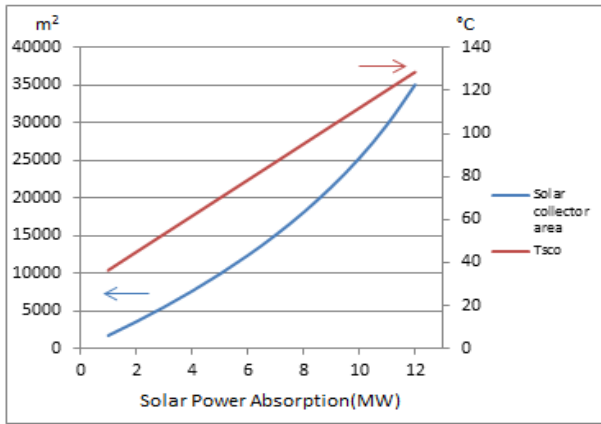**Figure 6** The solar power absorption as a function on net power output. (UA$_E$=UA$_C$=100kW)

Figure 7 The solar power absorption as a function of temperature and solar collector area. (UA_E=UA_C=100 kW)
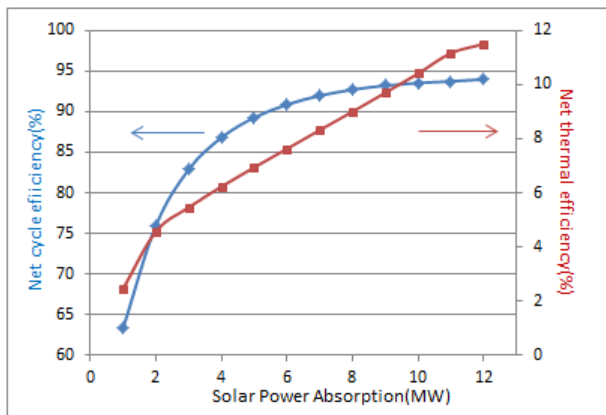

Figure 8 The net thermal efficiency and net cycle efficiency as a function of solar power absorption
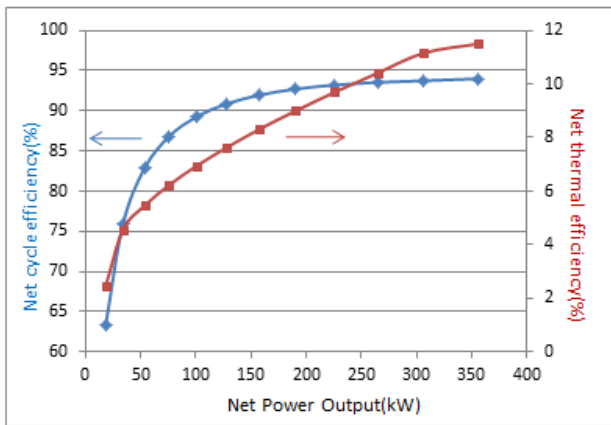

Figure 9 The net thermal efficiency and net cycle efficiency as a function of net power output

Figure 8 shows the simulation results for solar boosted OTEC system with various solar power absorption. In Figure 8 and 9, the simulation results are study based on the mass warm seawater flow rate equal to 30 kg/s. The net cycle efficiency is tends to increase in logarithmic-

like relationship with increasing the solar power absorption. Furthermore, the net thermal efficiency shows an upward graph pattern when solar power absorption increases from 1 MW to 12 MW. Increased solar power absorption will increase the temperature difference between warm and cold seawater. This in turn increases the enthalpy drop between point 1 and 2, causing the net power output to also increase. The highest net cycle efficiency achieved was 94% and it showed a larger reading of net power generation (i.e,360 kW). The net thermal efficiency achieved was 11.8% at the larger solar power absorption and net power output. When the solar thermal absorption reached 12 MW, the preheated seawater temperature reaches a point at which the net power output cannot increase any further unless the working fluid is superheated.
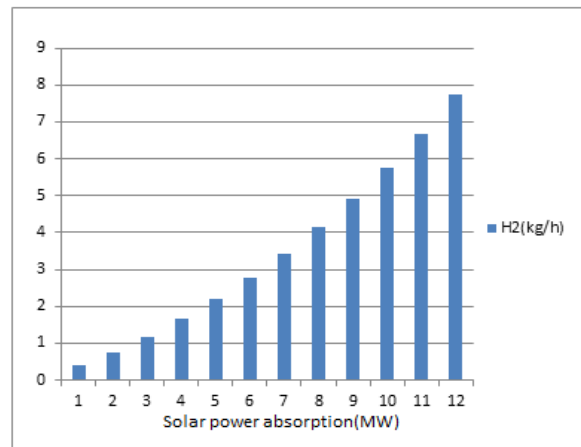

Figure 10 The hydrogen production as a function of solar power absorption

In this simulation study, the PEM electrolyzer is installed at the outlet of the turbine. The electricity that was produced from solar OTEC cycle is used to split the water molecules, thus generating hydrogen which then was stored in the available tank. Based on the recent study by Nidge University, the performance of PEM electrolyzer has been increased from 74% to 87% in a three year period due to great enhancement and development. The results showed in Figure 10 is based on the current efficiency of PEM electrolyzer which is 87%. To produce 1 kg/h of hydrogen gas requires about 40 kWh of electric power. Again it is very obvious that, increased in solar power absorption power will increase the hydrogen production.
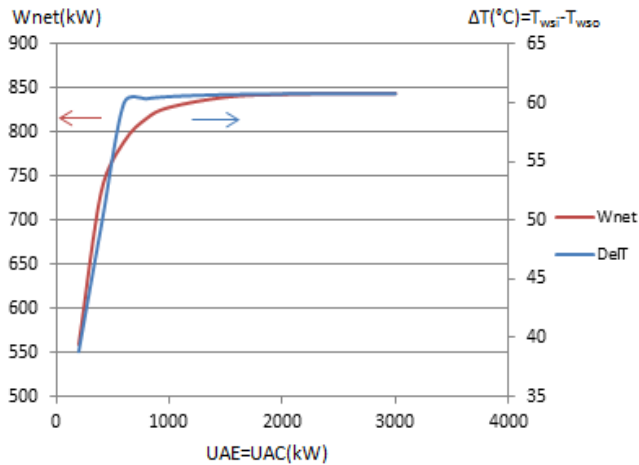
Figure 11 The relationship of overall heat transfer area of evaporator and condenser on net power generation and temperature difference.

As shown in Figure 11, the graph of net power output is increased until 845 kW when overall heat transfer area increased to 2000 kW/K. However, the pattern of the graph changed after that point and kept constant. This shows that, even if the overall heat transfer area keeps increasing, the net power output will increase only to a certain point and remain unchanged thereafter. Referring to the graph, for a larger value of overall heat transfer coefficient area indicate a higher temperature difference in order to get a maximum net power generation. However, at a temperature difference of 60°C and overall heat transfer coefficient area equal to 2000 kW/K, the net power output does not show any further changes. This shows that overall heat transfer coefficient area of 200kW/K will be sufficient to produce 845 kW of net power.

5.0 CONCLUSION

A solar boosted OTEC plant was used in this study and simulations involving several parameters were carried out. The results showed that adding solar collector at inlet of evaporator enhances the thermal efficiency of the conventional OTEC plant. The results also reveal that increasing the solar power absorption will increase the net power output and net thermal efficiency as well. Besides, hydrogen production also showed an increment when solar power absorb by solar collector increased. It is planned that in future studies, a more precise simulation including utilizing different types of working fluid will be conducted. Another consideration will be to carry out a variation of the study using superheated solar OTEC cycle. The results will provide insights from a thermodynamic perspective when combining sustainable energy with solar thermal energy to improve the system performance, which then indirectly increase the rate of hydrogen generated.

Acknowledgement

References

[1] Aydin, H., *et al*. 2014. Off-Design Performance Analysis of a Closed-cycle Ocean Thermal Energy Conversion System with Solar Thermal Preheating and Superheating. *Renewable Energy*. 72: 154-163.
[2] Wang, T., *et al*. 2010. Performance Analysis and Improvement for CC-OTEC System. *Journal of Mechanical Science and Technology*. 22(10): 1977-1983.
[3] Yeh, R.-H., T.-Z. Su, and M.-S. Yang. 2005. Maximum Output of an OTEC Power Plant. *Ocean Engineering*. 32(5-6): 685-700.
[4] Uehara, H. and Y. Ikegami. 1990. Optimization of a Closed-cycle OTEC System. *Journal of Solar Energy Engineering*. 112(4): 247-256.
[5] Ahmadi, P., I. Dincer, and M. A. Rosen. 2013. Energy and Exergy Analyses of Hydrogen Production Via Solar-Boosted Ocean Thermal Energy Conversion and PEM Electrolysis. *International Journal of Hydrogen Energy*. 38(4): 1795-1805.
[6] Yamada, N., A. Hoshi, and Y. Ikegami. 2009. Performance Simulation of Solar-boosted Ocean Thermal Energy Conversion Plant. *Renewable Energy*. 34(7): 1752-1758.
[7] Straatman, P. J. and W. G. van Sark. 2008. A New Hybrid Ocean Thermal Energy Conversion–Offshore Solar Pond (OTEC–OSP) Design: A Cost Optimization Approach. *Solar Energy*. 82(6): 520-527.
[8] Tinaikar, A. 2013. Ocean Thermal Energy Conversion. *International Journal of Energy and Power Engineering*. 2(4): 143.
[9] Uehara, H., *et al*. 1999. The Experimental Research on Ocean Thermal Energy Conversion Using the Uehara Cycle. In *Procedings of International OTEC/DOWA Conference, Imari, Japan*.
[10] Kalina, A. I. 1982. Generation of Energy by Means of a Working Fluid, and Regeneration of a Working Fluid. Google Patents.
[11] Ravindran, M. and R. Abraham. The Indian 1 MW Demonstration OTEC Plant and the Development Activities. In *OCEANS'02 MTS/IEEE*. 2002. IEEE.
[12] Dincer, I. 2012. Green Methods for Hydrogen Production. *International Journal of Hydrogen Energy*. 37(2): 1954-1971.
[13] Turner, J., *et al*. 2008. Renewable Hydrogen Production. *International Journal of Energy Research*. 32(5): 379-407.
[14] Nihous, G. and L. Vega. 1993. Design of a 100 MW OTEC-Hydrogen Plantship. *Marine Structures*. 6(2): 207-221.
[15] Vijayakrishna Rapaka, E., *et al*. *Modeling of Hydrogen Production through an Ocean Thermal Energy Conversion System*.